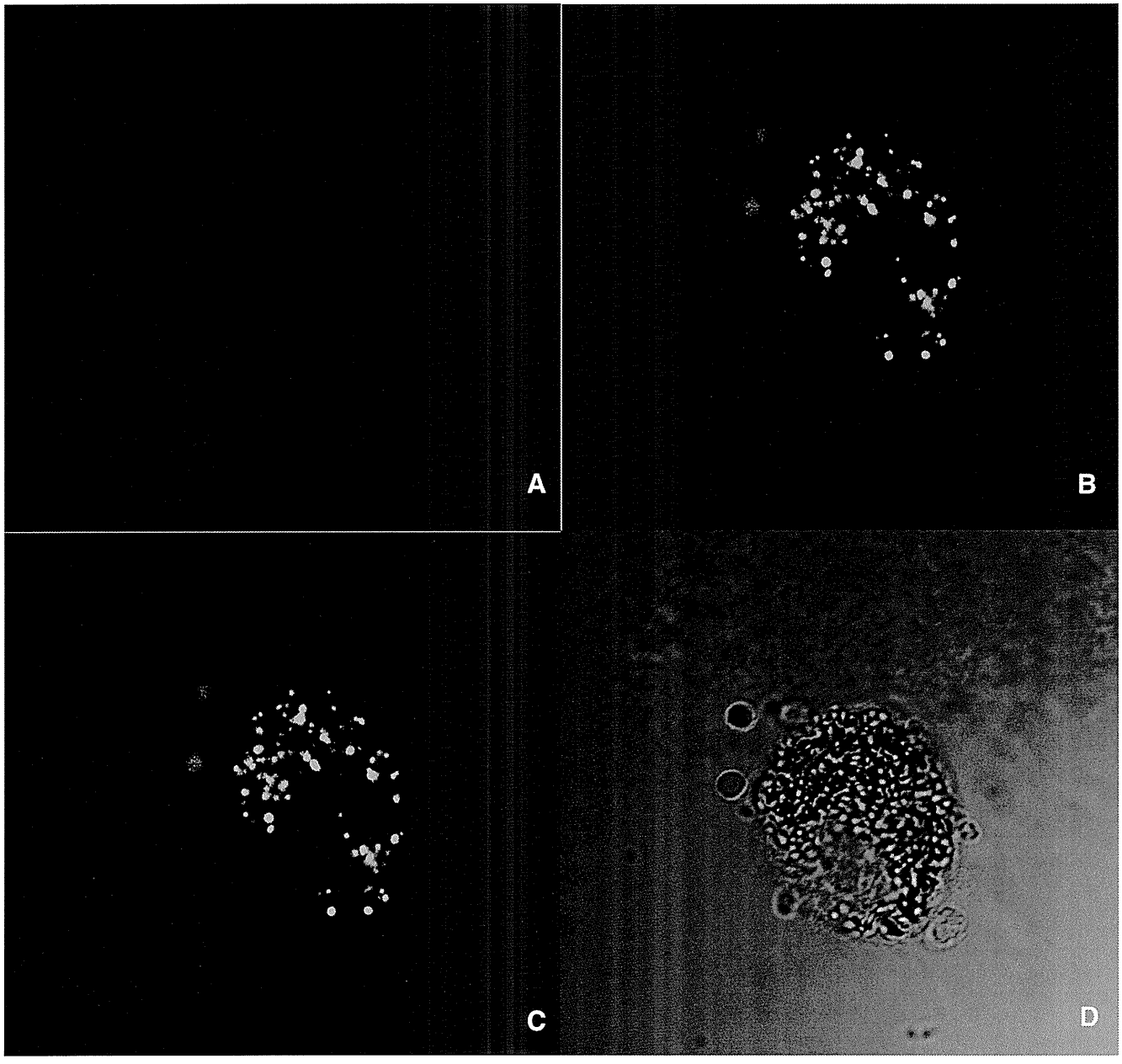

FIGURE 3. A cell obtained from the eye with rhegmatogenous retinal detachment shown in Figure 1 is negative for CD68 (**A**). Numerous small green autofluorescent inclusions in the cytoplasm were excited at 488 nm (**B**). (**A**) and (**B**) are superimposed in (**C**). The cytoplasm of the cell was filled with numerous pigment granules (**D**).

oma.[26] It has been speculated that the autofluorescent deposits may originate from macrophages.[8,10,14] However, little is known about autofluorescence of the macrophages in the subretinal space. In addition, although immunofluorescent staining of CD68 is frequently used as the cytomarker for macrophages in histologic study of the retina and the choroid, little information has been provided about autofluorescence of the CD68-positive cells in the eye. Thus, information about autofluorescence of the macrophages may help to interpret histologic results. In the present study, we investigated the autofluorescence properties of CD68-positive cells. AlexaFluor-647 was used as a secondary antibody dye to identify macrophages without interfering with observation of autofluorescence from the cells.

A case with subretinal precipitates in long-standing retinal detachment was reported by Vogt[27] in 1938. In such eyes, cytologic study has revealed that macrophages are the dominant cell population in the subretinal fluid.[28,29] Coats' disease is a retinal vascular disease showing yellow golden deposits in the retina[30] and bullous retinal detachment occasionally. Numerous macrophages were confirmed in the subretinal fluid aspirated from the eyes with retinal detachment.[21,31] Abnormal FAF in both diseases has not been reported. We noticed hyperautofluorescent deposits corresponding to subretinal precipitates in the eyes with RRD and spotted hyperautofluorescence in the area of retinal detachment caused by Coats' disease. In the eyes with RRD, hyperautofluorescence appeared along subretinal strands. Previous histopathologic studies suggested that subretinal strands are composed of macrophage and retinal pigment epithelium.[32–35] Macrophages may have a part in the origin of subretinal strands.

Three types of cells were morphologically identified in the subretinal fluid from the four eyes in the present study. Immuno-

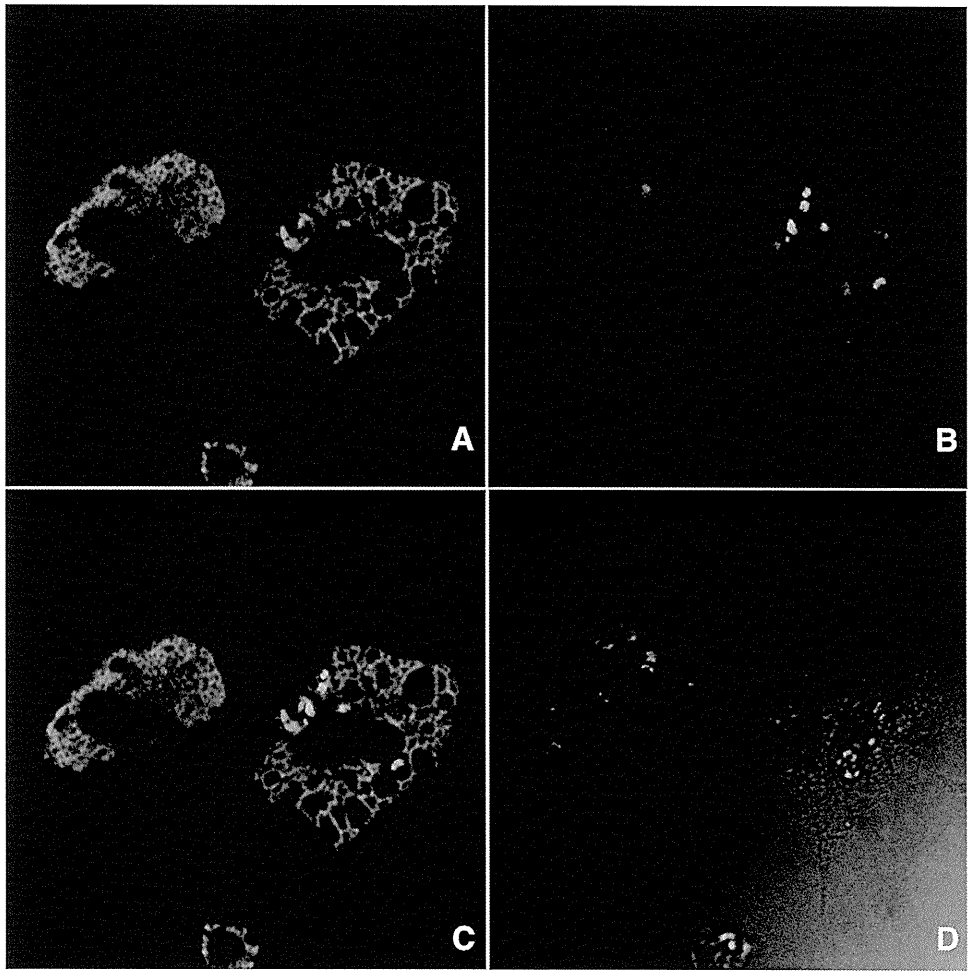

FIGURE 4. This cell was obtained from the eye with exudative retinal detachment shown in Figure 2. Polygonal large cells with numerous vacuoles were positive for CD68 (**A**). Green autofluorescent inclusions were excited by a 488-nm laser light (**B**). (**A**) and (**B**) are superimposed. Autofluorescent inclusions were observed in the vacuoles and cytoplasm (**C**). In some cells, few pigment granules were found (**D**).

fluorescent staining confirmed that most of the lightly pigmented large cells were CD68-positive macrophages. Pigmented CD68-negative cells, on the other hand, were considered likely to be derived from the retinal pigment epithelium, because of their morphologic characteristics. Since autofluorescence appeared only in these types of cells, they were possible origins of abnormal autofluorescence in the subretinal space.

Peak analysis for 50 inclusions consistently showed similar fluorescence properties, suggesting that the inclusions in both types of cells may have similar composition of fluorescent material. Autofluorescent inclusions in both types of cells showed yellow-red peak emissions within the range of 558 to 612 nm (Fig. 6). Consistent with this observation, ex vivo experiments of the human retinal pigment epithelium showed that the peak emission of lipofuscin appeared within the range of 588 to 610 nm.[36] Peak emission of lipofuscin varies by age,[25,37] physical condition,[38] and method of extraction. Consideration of variation of emission spectra of lipofuscin from these reports suggests that yellow-red emission originates from lipofuscin-like materials in the cells. Previously, lipofuscin was considered to be synthesized in the retinal pigment epithelium as a product of phagocytosis of the photoreceptor outer segments. Recent reports have suggested that A2E and its derivatives are synthesized in the photoreceptor outer segments before phagocytosis by the retinal pigment epithelium.[39] Lipofuscin-like materials could also accumu-

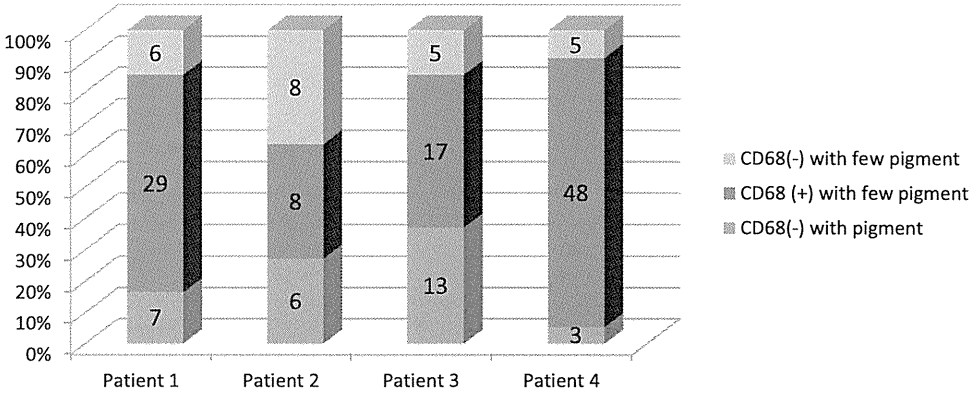

FIGURE 5. The cell density of each type of the cells. The number of cells in four microscopic fields when 40× object lens was used. Total area of counting cells was approximately 0.1024 mm^3.

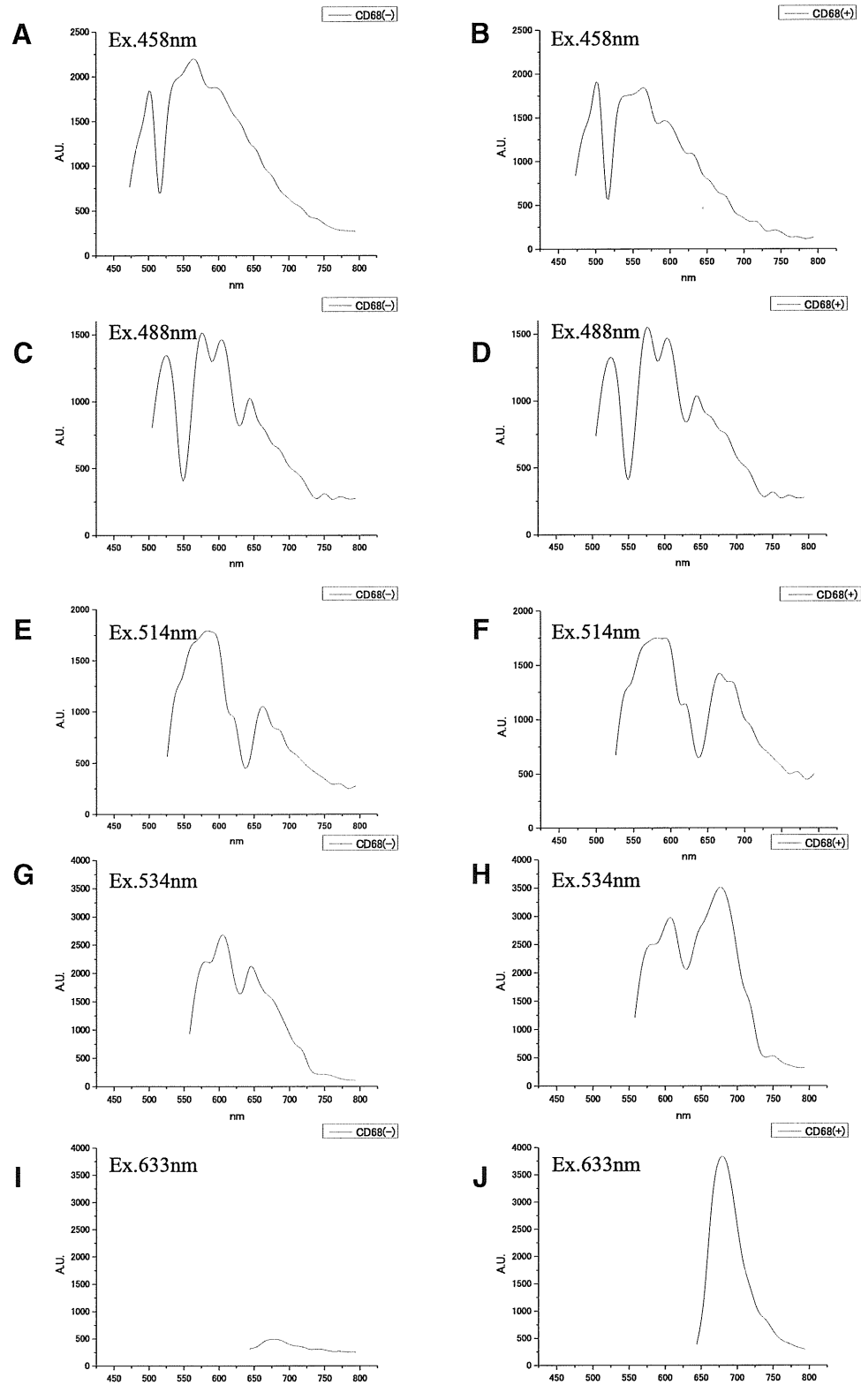

Figure 6. Fluorescence emission fingerprints of CD68-negative and -positive cells collected from subretinal fluid in the eye with rhegmatogenous retinal detachment. (**A**, **C**, **E**, **G**, **I**) the CD68-negative cells; (**B**, **D**, **F**, **H**, **J**) the CD68-positive cells. Ex: Excitation wavelengths: 458, 488, 514, 534, and 633 nm, respectively (*top* to *bottom*).

late in the macrophages. Specifically, the accumulated outer segment material in phagosomes in the macrophages may generate autofluorescence similar to that in the retinal pigment epithelium. Since the former two types of cells showed autofluorescence in the cells, they were considered to be the source of subretinal autofluorescence in part. Autofluorescence was observed in the phagosomal vacuole. Hence, autofluorescent substances may have already been synthesized in shed outer segments before phagocytosis. Recent reports have also raised this possibility.[14,39] However, autofluorescence characteristics of shed substances in the subretinal space are still unknown. Further study is needed of this phenomenon.

The digested photoreceptor outer segments that may not be properly processed in the macrophages may become lipofuscin. The possibility of the photoreceptor outer segments being

TABLE 2. Peak Analysis of the 50 Inclusions in the CD68-negative and -positive Cells

Emission Wavelength (NM)	CD68	Excitation Wavelength (nm) 458 (−)	458 (+)	488 (−)	488 (+)	514 (−)	514 (+)	543 (−)	543 (+)	633 (−)	633 (+)
462		0	—	—	—	—	—	—	—	—	—
473		0	0	—	—	—	—	—	—	—	—
483		0	0	—	—	—	—	—	—	—	—
494		3	0	—	—	—	—	—	—	—	—
505		45	50	0	0	—	—	—	—	—	—
515		0	0	0	0	—	—	—	—	—	—
526		0	0	50	50	0	0	—	—	—	—
537		2	1	0	0	0	0	—	—	—	—
547		1	1	0	0	0	0	—	—	—	—
558		39	33	0	0	1	0	0	0	—	—
569		8	16	0	0	4	5	0	0	—	—
580		0	0	39	44	21	25	0	1	—	—
590		0	0	0	0	25	20	0	0	—	—
601		0	0	11	6	0	0	29	23	—	—
612		0	0	0	0	0	0	21	27	—	—
622		0	0	0	0	0	0	0	0	—	—
633		0	0	0	0	0	0	0	0	—	—
644		0	0	45	50	0	0	46	1	0	0
654		0	0	0	0	1	0	3	0	0	0
665		0	0	0	0	49	49	0	0	0	0
676		0	0	0	0	0	1	0	50	47	50
687		0	0	0	0	0	0	0	0	3	0
697		0	0	0	0	0	0	0	0	0	0
708		0	0	0	0	0	0	0	0	0	0
‖		‖	‖	‖	‖	‖	‖	‖	‖	‖	‖
794		0	0	0	0	0	0	0	0	0	0

processed into autofluorescent material in the subretinal macrophages could not be excluded.

CD68-positive cells showed two autofluorescence peaks within the range of 480 to 750 nm. In the present study, green emission peaks of autofluorescence, 505 nm for 457-nm excitation and 526 nm for 488-nm excitation, were observed. This emission spectrum was reported to appear in living human eyes.[37,40] Flavin adenine dinucleotide (FAD) is considered to be the main source of the green emission. In the 488-nm emission spectra, the narrow peak appeared around 520 nm (Figs. 6C, 6D). A similar peak also appeared on the left shoulder of the broad peak (right), straddling 530 to 535 nm along the *x*-axis in the spectra induced by 458-nm light (Figs. 6A, 6B). The flavoprotein signal may be incorporated into this peak.[41] Since the green emission was not observed in macrophages in the lung[42] or peripheral blood,[43] the fluorophore would be distinctive to macrophages in the subretinal space. Why would this emission spectrum appear only in the inclusions of the macrophages in the subretinal space? Macrophages accumulate in the outer nuclear layer in regions of ongoing rod cell death after retinal detachment.[44] Degenerated photoreceptor cells may be phagocytized by the macrophages. The highest concentration of FAD is found in the mitochondria of the photoreceptor's inner segments. As the results of phagocytosis, the mitochondria of the photoreceptor cells may accumulate in the phagosomes of macrophages and show green emission autofluorescence. Therefore, the macrophages in the subretinal space in eyes with retinal detachment would be predicted to show that green and yellow autofluorescence originates from lipofuscin-like materials and FAD. Inclusions in cells of the mouse models of age-related macular degeneration showed a spectrum similar to that of our samples.[45] The increase in autofluorescence in an elderly population and patients with macular degeneration may reflect autofluorescence from macrophages associated with photoreceptor death.

In this study, we were unable to determine the chemical composition of autofluorescent substances, since the quantity of cells obtained from surgically removed subretinal fluid was limited. Further study is needed to examine whether the subretinal inclusions have the same composition as lipofuscin or FAD.

With regard to the origins of CD68-positive cells, we should use the other antibodies that are more specific for tissue macrophages. A minority of the retinal pigment epithelium has been reported to be CD68-positive in situ.[46] The transformation of the retinal pigment epithelium into the macrophages is assumed to be one source of the subretinal macrophages.[47] CD68-positive retinal pigment epithelial cells may look morphologically similar to macrophages. Therefore, the CD68-positive cells include the tissue macrophages and the transformed retinal pigment epithelium. To determine the contribution of the tissue macrophage to autofluorescence in the subretinal space, more specific staining is needed. However, the broad spectrum of autofluorescence and small amount of the specimens did not allow us to perform multiple staining. Further study of this issue is need.

In conclusion, we found that inclusions in the macrophages in the subretinal space emit intense autofluorescence. The spectra of the autofluorescence are very similar to that of the retinal pigment epithelium. Hence, autofluorescent properties of deposits in subretinal space raise the possibility that they are macrophages, and further critical markers are needed for clinical assessment as to their identity.

References

1. Eldred GE, Lasky MR. Retinal age pigments generated by self-assembling lysosomotropic detergents. *Nature.* 1993;361:724–726.
2. Liu J, Itagaki Y, Ben-Shabat S, Nakanishi K, Sparrow JR. The biosynthesis of A2E, a fluorophore of aging retina, involves the for-

mation of the precursor, A2-PE, in the photoreceptor outer segment membrane. *J Biol Chem.* 2000;275:29354-29360.
3. Parish CA, Hashimoto M, Nakanishi K, Dillon J, Sparrow J. Isolation and one-step preparation of A2E and iso-A2E, fluorophores from human retinal pigment epithelium. *Proc Natl Acad Sci U S A.* 1998;95:14609-14613.
4. Spaide RF, Noble K, Morgan A, Freund KB. Vitelliform macular dystrophy. *Ophthalmology.* 2006;113:1392-1400.
5. Chung JE, Spaide RF. Fundus autofluorescence and vitelliform macular dystrophy. *Arch Ophthalmol.* 2004;122:1078-1079.
6. Framme C, Walter A, Gabler B, Roider J, Sachs HG, Gabel VP. Fundus autofluorescence in acute and chronic-recurrent central serous chorioretinopathy. *Acta Ophthalmol Scand.* 2005;83:161-167.
7. Kon Y, Iida T, Maruko I, Saito M. The optical coherence tomography-ophthalmoscope for examination of central serous chorioretinopathy with precipitates. *Retina.* 2008;28:864-869.
8. Maruko I, Iida T, Ojima A, Sekiryu T. Subretinal dot-like precipitates and yellow material in central serous chorioretinopathy. *Retina.* 2011;31:759-765.
9. Sasamoto Y, Gomi F, Sawa M, Tsujikawa M, Hamasaki T. Macular pigment optical density in central serous chorioretinopathy. *Invest Ophthalmol Vis Sci.* 2010;51:5219-5225.
10. Sekiryu T, Iida T, Maruko I, Saito K, Kondo T. Infrared fundus autofluorescence and central serous chorioretinopathy. *Invest Ophthalmol Vis Sci.* 2010;51:4956-4962.
11. Spaide RF, Klancnik JM Jr. Fundus autofluorescence and central serous chorioretinopathy. *Ophthalmology.* 2005;112:825-833.
12. Shields CL, Bianciotto C, Pirondini C, Materin MA, Harmon SA, Shields JA. Autofluorescence of orange pigment overlying small choroidal melanoma. *Retina.* 2007;27:1107-1111.
13. Koizumi H, Maruyama K, Kinoshita S. Blue light and near-infrared fundus autofluorescence in acute Vogt-Koyanagi-Harada disease. *Br J Ophthalmol.* 2010;94:1499-1505.
14. Spaide R. Autofluorescence from the outer retina and subretinal space: hypothesis and review. *Retina.* 2008;28:5-35.
15. Weingeist TA, Kobrin JL, Watzke RC. Histopathology of Best's macular dystrophy. *Arch Ophthalmol.* 1982;100:1108-1114.
16. Schachat AP, de la Cruz Z, Green WR, Patz A. Macular hole and retinal detachment in Best's disease. *Retina.* 1985;5:22-25.
17. Kamei M, Yoneda K, Kume N, et al. Scavenger receptors for oxidized lipoprotein in age-related macular degeneration. *Invest Ophthalmol Vis Sci.* 2007;48:1801-1807.
18. Grossniklaus HE, Miskala PH, Green WR, et al. Histopathologic and ultrastructural features of surgically excised subfoveal choroidal neovascular lesions: submacular surgery trials report no. 7. *Arch Ophthalmol.* 2005;123:914-921.
19. Herbert EN, Sheth HG, Wickremasinghe S, Luthert PJ, Bainbridge J, Gregor ZJ. Nature of subretinal fluid in patients undergoing vitrectomy for macular hole: a cytopathological and optical coherence tomography study. *Clin Exp Ophthalmol.* 2008;36:812-816.
20. Baudouin C, Hofman P, Brignole F, Bayle J, Loubiere R, Gastaud P. Immunocytology of cellular components in vitreous and subretinal fluid from patients with proliferative vitreoretinopathy. *Ophthalmologica.* 1991;203:38-46.
21. Kremer I, Nissenkorn I, Ben-Sira I. Cytologic and biochemical examination of the subretinal fluid in diagnosis of Coats' disease. *Acta Ophthalmol (Copenh).* 1989;67:342-346.
22. Lai WW, Leung GY, Chan CW, Yeung IY, Wong D. Simultaneous spectral domain OCT and fundus autofluorescence imaging of the macula and microperimetric correspondence after successful repair of rhegmatogenous retinal detachment. *Br J Ophthalmol.* 2010;94:311-318.
23. Ojima A, Iida T, Sekiryu T, Maruko I, Sugano Y. Photopigments in central serous chorioretinopathy. *Am J Ophthalmol.* 2011;151:940-952 e941.
24. Miller SA. Fluorescence in Best's vitelliform dystrophy, lipofuscin, and fundus flavimaculatus. *Br J Ophthalmol.* 1978;62:256-260.
25. Delori FC, Fleckner MR, Goger DG, Weiter JJ, Dorey CK. Autofluorescence distribution associated with drusen in age-related macular degeneration. *Invest Ophthalmol Vis Sci.* 2000;41:496-504.
26. Ramasubramanian A, Shields CL, Harmon SA, Shields JA. Autofluorescence of choroidal hemangioma in 34 consecutive eyes. *Retina.* 2010;30:16-22.
27. Vogt A. Ueber subvaskulare Weissfleckung der abgelosten retina, von der Form von weissen Prazipitaten. *Klin Monatsbl Augenheilkd,* 1938;101:864-866.
28. Robertson DM. Delayed absorption of subretinal fluid after scleral buckling procedures: the significance of subretinal precipitates. *Trans Am Ophthalmol Soc.* 1978;76:557-583.
29. Toti P, Morocutti A, Sforzi C, De Santi MM, Catella AM, Baiocchi S. The subretinal fluid in retinal detachment: a cytologic study. *Doc Ophthalmol.* 1991;77:39-46.
30. Shields JA, Shields CL. Review: coats disease: the 2001 LuEsther T. Mertz lecture. *Retina.* 2002;22:80-91.
31. Haik BG, Koizumi J, Smith ME, Ellsworth RM. Fresh preparation of subretinal fluid aspirations in Coats' disease. *Am J Ophthalmol.* 1985;100:327-328.
32. Matsumura M, Yamakawa R, Yoshimura N, Shirakawa H, Okada M, Ogino N. Subretinal strands: tissue culture and histological study. *Graefes Arch Clin Exp Ophthalmol.* 1987;225:341-345.
33. Mietz H, Stodtler M, Wiedemann P, Heimann K. Immunohistochemistry of cellular proliferation in eyes with longstanding retinal detachment. *Int Ophthalmol.* 1994;18:329-337.
34. Okada M, Ogino N, Matsumura M, Honda Y, Nagai Y. The process of subretinal strand formation. *Jpn J Ophthalmol.* 1992;36:222-234.
35. Trese MT, Chandler DB, Machemer R. Subretinal strands: ultrastructural features. *Graefes Arch Clin Exp Ophthalmol.* 1985;223:35-40.
36. Delori FC, Dorey CK, Staurenghi G, Arend O, Goger DG, Weiter JJ. In vivo fluorescence of the ocular fundus exhibits retinal pigment epithelium lipofuscin characteristics. *Invest Ophthalmol Vis Sci.* 1995;36:718-729.
37. Boulton M, Docchio F, Dayhaw-Barker P, Ramponi R, Cubeddu R. Age-related changes in the morphology, absorption and fluorescence of melanosomes and lipofuscin granules of the retinal pigment epithelium. *Vision Res.* 1990;30:1291-1303.
38. Haralampus-Grynaviski NM, Lamb LE, Clancy CM, et al. Spectroscopic and morphological studies of human retinal lipofuscin granules. *Proc Natl Acad Sci U S A.* 2003;100:3179-3184.
39. Sparrow JR, Wu Y, Nagasaki T, Yoon KD, Yamamoto K, Zhou J. Fundus autofluorescence and the bisretinoids of retina. *Photochem Photobiol Sci.* 2010;9:1480-1489.
40. Elner SG, Elner VM, Field MG, Park S, Heckenlively JR, Petty HR. Retinal flavoprotein autofluorescence as a measure of retinal health. *Trans Am Ophthalmol Soc.* 2008;106:215-222; discussion 222-214.
41. Benson RC, Meyer RA, Zaruba ME, McKhann GM. Cellular autofluorescence: is it due to flavins? *J Histochem Cytochem.* 1979;27:44-48.
42. Pauly JL, Allison EM, Hurley EL, Nwogu CE, Wallace PK, Paszkiewicz GM. Fluorescent human lung macrophages analyzed by spectral confocal laser scanning microscopy and multispectral cytometry. *Microsc Res Tech.* 2005;67:79-89.
43. Davis RW, Timlin JA, Kaiser JN, Sinclair MB, Jones HD, Lane TW. Accurate detection of low levels of fluorescence emission in autofluorescent background: francisella-infected macrophage cells. *Microsc Microanal.* 2010;16:478-487.
44. Nakazawa T, Takeda M, Lewis GP, et al. Attenuated glial reactions and photoreceptor degeneration after retinal detachment in mice deficient in glial fibrillary acidic protein and vimentin. *Invest Ophthalmol Vis Sci.* 2007;48:2760-2768.
45. Xu H, Chen M, Manivannan A, Lois N, Forrester JV. Age-dependent accumulation of lipofuscin in perivascular and subretinal microglia in experimental mice. *Aging Cell.* 2008;7:58-68.
46. Elner SG, Elner VM, Nielsen JC, Torczynski E, Yu R, Franklin WA. CD68 antigen expression by human retinal pigment epithelial cells. *Exp Eye Res.* 1992;55:21-28.
47. Mandelcorn MS, Machemer R, Fineberg E, Hersch SB. Proliferation and metaplasia of intravitreal retinal pigment epithelium cell autotransplants. *Am J Ophthalmol.* 1975;80:227-237.

Photopigments in Central Serous Chorioretinopathy

AKIRA OJIMA, TOMOHIRO IIDA, TETSUJU SEKIRYU, ICHIRO MARUKO, AND YUKINORI SUGANO

• PURPOSE: To investigate functional abnormalities in eyes with central serous chorioretinopathy (CSC).
• DESIGN: Observational case series.
• METHODS: Sixteen eyes with CSC were enrolled. Autofluorescence densitometry was performed to measure the optical density of the photopigments. Serial fundus autofluorescence (FAF) images were obtained by Heidelberg Retina Angiogram 2. We calculated the autofluorescence optical density difference from the FAF images. To compare the distribution pattern of autofluorescence optical density difference to the findings of outer retina, spectral-domain optical coherence tomography (SD-OCT) was performed in the acute phase and after resolution of CSC.
• RESULTS: The autofluorescence optical density difference decreased at the serous retinal detachment (SRD) in all 16 eyes. After resolution, the photoreceptor inner and outer segment junction (IS/OS) was irregular in 13 eyes and defective in 3 eyes on SD-OCT. The autofluorescence optical density difference did not improve in any eyes. Five eyes were reexamined 3 month after resolution. In 4 of the 5 eyes, SD-OCT showed that the IS/OS was well delineated and 1 eye defective. The autofluorescence optical density difference improved in 2 of the 4 eyes, but not in the other 2 eyes. In the 1 eye without well-delineated IS/OS, the autofluorescence optical density difference did not improve.
• CONCLUSION: In eyes with CSC, the photopigment density decreased at the SRD. The density remained decreased immediately after resolution and showed delayed recovery. The photopigments decreased even in eyes with morphologic recovery of the outer retina. (Am J Ophthalmol 2011;151:940–952. © 2011 by Elsevier Inc. All rights reserved.)

CENTRAL SEROUS CHORIORETINOPATHY (CSC) IS characterized by serous retinal detachment (SRD) in the macular area. Focal dye leakage at the level of the retinal pigment epithelium (RPE) is seen on fluorescein angiography. In most eyes, the SRD resolves spontaneously, and the visual acuity (VA) recovers fully in these eyes. However, patients often complain about relative scotoma, abnormal color sensation, and micropsia despite resolution of the SRD.

Accepted for publication Dec 3, 2010.

From the Department of Ophthalmology, Fukushima Medical University School of Medicine, Fukushima, Japan.

Inquiries to Akira Ojima, Department of Ophthalmology, Fukushima Medical University School of Medicine, 1 Hikarigaoka, Fukushima, Japan; e-mail: ao@fmu.ac.jp

Morphologic retinal abnormalities in CSC have been observed on optical coherence tomography (OCT).[1–8] In the acute phase of CSC, thickened neurosensory retina and elongated photoreceptor outer segments are seen at the area of the SRD.[1–8] In the quiescent phase, defects of the photoreceptor inner and outer segment junction (IS/OS) are sometimes seen.[4] Thinning of the outer photoreceptor layer and the defects in the subfoveal IS/OS may be associated with VA loss.[2,4,8]

Some studies using microperimetry have reported that retinal sensitivity was attenuated in eyes with CSC even after resolution of the SRD.[9,10] Spectral-domain OCT (SD-OCT) showed loss of retinal sensitivity in areas with an irregular RPE or a defect of the IS/OS.[10] Reduced amplitudes of the multifocal electroretinogram were observed not only in the acute phase but also after resolution of the SRD.[11,12] Although these functional disorders seem to be associated with loss of the IS/OS or RPE atrophy, some patients complain about blurred vision even after complete morphologic recovery of the IS/OS. The role of the OCT findings in visual function is uncertain. In these cases, functional impairment might be attributed to decreases in the visual photopigments.

Retinal densitometry is the only objective method for investigating visual photopigments in vivo.[13–22] Liem and associates,[23] using reflective densitometry in eyes with CSC, reported that the rhodopsin concentration decreased in the area of the SRD. Since that method requires special equipment, it is not used clinically.

In a previous study, we reported other methods of retinal densitometry using the fundus autofluorescence (FAF) examination by commercially available scanning laser ophthalmoscope.[24] We recorded serial FAF images using the Heidelberg Retina Angiogram 2 (HRA2; Heidelberg Engineering, Dossenheim, Germany), and calculated the photopigment density from the time-dependent changes in intensity of FAF during excitation. We named the technique autofluorescence densitometry. The density is measured as the autofluorescence optical density difference of the photopigments. This new technique can examine a much broader macular area than in previous studies and create a distribution map of optical density of the photopigments. It is also easy to compare the distributions of the photopigment densities with other retinal imaging devices such as SD-OCT. We used autofluorescence densitometry to evaluate changes in the photopigments in acute and quiescent phase of CSC.

0002-9394/$36.00
doi:10.1016/j.ajo.2010.12.005

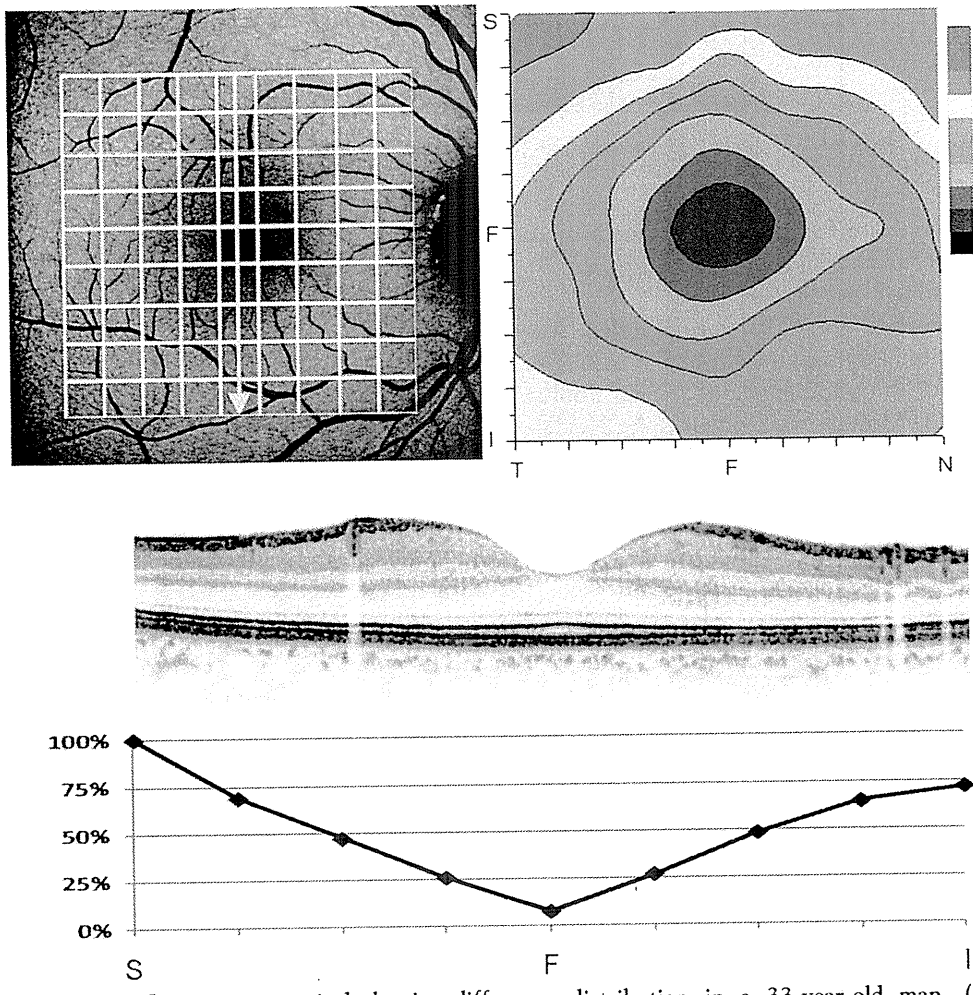

FIGURE 1. A normal autofluorescence optical density difference distribution in a 33-year-old man. (Top left) Fundus autofluorescence image. The intensity of each point on the grids was measured to calculate the autofluorescence optical density difference. The arrow indicates the line of the spectral-domain optical coherence tomography (SD-OCT) scan. (Top right) A normal autofluorescence optical density difference map has a concentric pattern. S = superior; F = fovea; I = inferior; T = temporal; N = nasal. (Middle) A vertical SD-OCT scan shows a normal layer structure. (Bottom) The % autofluorescence optical density difference graph at the SD-OCT scan line. The abscissa indicates the position.

METHODS

AMONG 26 CONSECUTIVE PATIENTS WITH CSC EXAMINED by both autofluorescence densitometry and SD-OCT, 16 eyes of 16 patients were included in this study (14 men, 2 women; mean age, 50.1 years; range, 31–71 years). All patients visited the Department of Ophthalmology at Fukushima Medical University Hospital between August 1, 2008 and May 31, 2009. The 16 eyes met the following criteria: the maximum diameter of the SRD exceeded 3 disc diameters including the fovea; autofluorescence densitometry was performed during the acute and quiescent phases; and resolution of the SRD was observed on SD-OCT during the follow-up period. The remaining 10 patients did not meet these criteria. In the 10 patients who were excluded, 8 patients had small SRD with maximum diameter less than 3 disc diameters, and 2 patients could not be followed up.

All patients underwent a comprehensive ophthalmologic examination, including measurement of the best-corrected VA, slit-lamp biomicroscopy, fundus photography, fluorescein angiography, SD-OCT, and FAF. The best-corrected VA was measured with a Japanese standard decimal visual chart and converted to logarithm of the minimal angle of resolution for statistical analysis. SD-OCT was performed with a 3-dimensional OCT system (Topcon, Tokyo, Japan) or Spectralis OCT system (Heidelberg Engineering, Heidelberg, Germany). The diagnosis of CSC was confirmed by the presence of a macular SRD and leakage from the level of the RPE on fluorescein angiography. Patients with other pathologies that can cause retinal detachment, such as age-related macular degeneration, Harada's disease, posterior scleritis, and any other macular diseases, were excluded. All data were collected prospectively and reviewed in a masked fashion.

We also examined 10 control subjects (mean age, 40 years; age range, 31–55 years) who were free from retinal

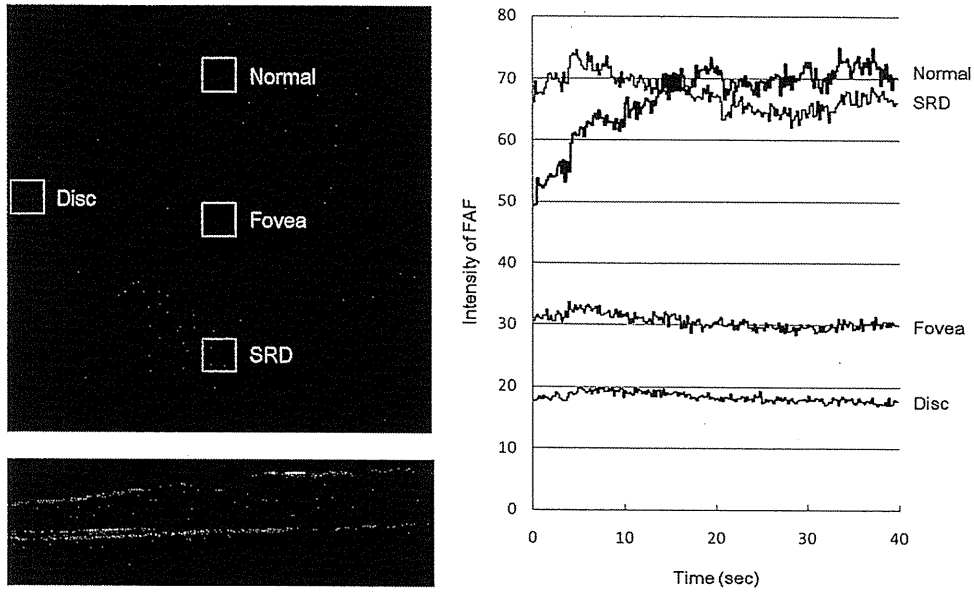

FIGURE 2. Changes in fundus autofluorescence (FAF) intensity in the left eye of a 37-year-old man with acute central serous chorioretinopathy (Patient 4). (Top left) FAF image. The mean intensity within each area was measured. The squares indicate the area of measurement. Normal, the area without a serous retinal detachment (SRD); SRD, the area within an SRD. (Bottom left) A vertical spectral-domain optical coherence tomography scan shows an SRD. (Right) Time-dependent changes in the FAF intensity during light exposure. The intensity increased in the normal area because of bleaching of the retina. The area with an SRD does not have increased FAF. The increases in FAF intensity indicate the presence of normal photopigments. The change in intensity is low at the fovea, because the excitation light is attenuated by macular pigment. The autofluorescence optical density difference cannot be evaluated accurately at the fovea. The FAF intensity is very low and does not change by light exposure at the disc.

diseases, significant cataract, or corneal opacity. All subjects underwent the same examination as above except for fluorescein angiography.

Patients who needed good vision because of their occupations or desired treatment underwent laser photocoagulation after being informed of the risks and benefits. Treatment was performed using a DPSS yellow laser (561 nm; Nidek, Gamagori, Japan) with a spot size of 200 μm, power of 70 to 100 mW, and application time of 0.20 second. The endpoint of laser photocoagulation was slight graying of the RPE.

The autofluorescence optical density difference of the photopigments was measured repeatedly by the autofluorescence densitometry technique of the FAF examination to investigate time-dependent changes. We also evaluated the morphologic changes of the outer retina on the horizontal and vertical images of the SD-OCT. The area of interest was examined by raster scan. We classified the OCT findings of IS/OS in the area of SRD into 3 groups: clear, irregular, and defect. "Clear" indicates normal IS/OS line; "irregular" is discontinuous or blurred IS/OS line; "defect" means lack of IS/OS line.

The autofluorescence densitometry technique was described previously.[19] The FAF images were recorded using HRA2. After pupil dilation with topical tropicamide and phenylephrine, the patients were dark-adapted for at least 30 minutes before the examination. Serial FAF images were obtained over 40 seconds using high-speed movie mode. The angle of field was 30 degrees. The intensity of excitation was 100% and the gain was 94%. The FAF images were aligned to fix the viewpoint using the software in the HRA2 system and were output as audio video interleaved (AVI) files for measurement. We measured the distribution of the FAF intensity in a 6 × 6-mm-square area around the fovea. The area was divided into 9 × 9 grids, and the intensity of each point was measured as an 8-bit grayscale value on the frame of the AVI files (Gray-val; Library Inc, Tokyo, Japan).

To estimate the autofluorescence optical density difference of the photopigments, the grayscale value during light exposure was fitted to the following formula. The intensity of the FAF at time t was described as:

$$\log[F(t)] = \log[F(\infty)] - \mathrm{fODD} \times \exp(-kt)$$

where $F(t)$ is the measured autofluorescence at time t, $F(\infty)$ is the autofluorescence at an infinite time when the $F(t)$ approaches a constant level, fODD is the optical density difference of the pigment between the dark-adapted density and the density of the pigment after an infinitely long duration, and k is the time constant relating the chromophore properties and the intensity of light at the measurement site. We fitted the value of the FAF intensity to the equation on a least-squares basis with the Levenberg-Marquardt method, which provides the 3 unknown parameters ($\log[F(\infty)]$, fODD, and k), using Origin 8.0 computer software (OriginLab Corporation,

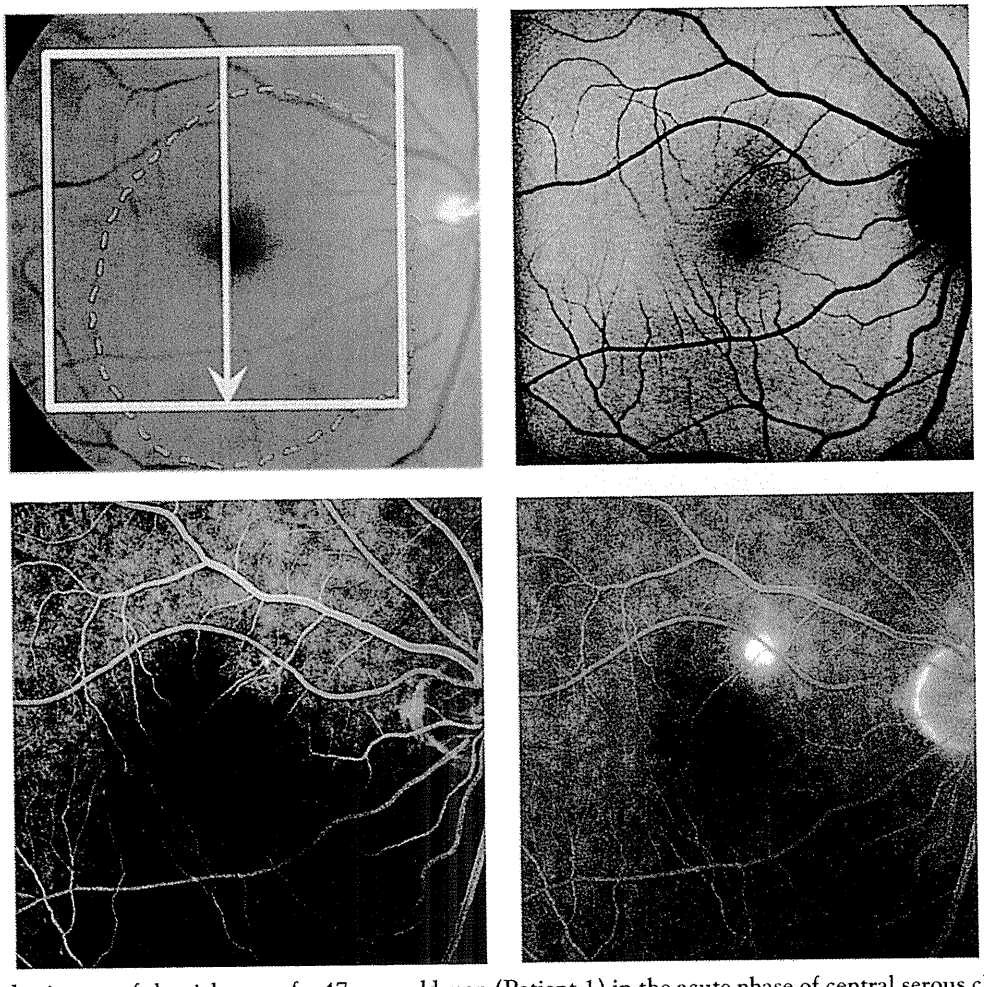

FIGURE 3. Fundus images of the right eye of a 47-year-old man (Patient 1) in the acute phase of central serous chorioretinopathy. (Top left) Fundus photograph. The square indicates the area in which the autofluorescence optical density difference was measured (see Figure 4). The dashed line shows the area of the serous retinal detachment. The yellow arrow indicates the scanning line of spectral-domain optical coherence tomography (see Figure 4). (Top right) Fundus autofluorescence image. (Bottom) Focal dye leakage is seen in (Bottom left) the early phase and (Bottom right) the late phase of the fluorescein angiograms.

Northampton, Massachusetts, USA). The results were displayed using a contour map classified into 11 phases (autofluorescence optical density difference map). When the intensity of the autofluorescence decreased or the change in the autofluorescence intensity was too small to fit the equation at the measurement site, the autofluorescence optical density difference of the site was treated as zero.

RESULTS

THE TABLE SHOWS THE CLINICAL PATIENT PROFILES. THE duration of symptoms from the subjective onset ranged from 1 to 49 months (mean, 10.4 months). Six patients with symptom duration of more than 6 months were diagnosed with chronic CSC. The other 16 patients were diagnosed with acute CSC.

In the current study, we observed all 16 eyes in the acute phase and immediately after resolution of the SRD. Five of the 16 eyes were reexamined 3 months after resolution. All eyes in the acute phase had focal leakage at the macular area on fluorescein angiography and a SRD that included the fovea. Eleven of the 16 eyes had an elongated photoreceptor outer segment on SD-OCT. Twelve of the 16 eyes were treated with laser photocoagulation. The SRDs resolved on SD-OCT between 3 and 54 months (mean, 13.4 months) from the subjective onset of symptoms.

The autofluorescence optical density difference map showed a concentric pattern in all 10 control subjects. Figure 1 shows a normal autofluorescence optical density difference map of a healthy subject (33-year-old man). All FAF and SD-OCT findings were normal (Figure 1, Top left, Middle). To calculate the autofluorescence optical density difference, time-dependent changes in the FAF

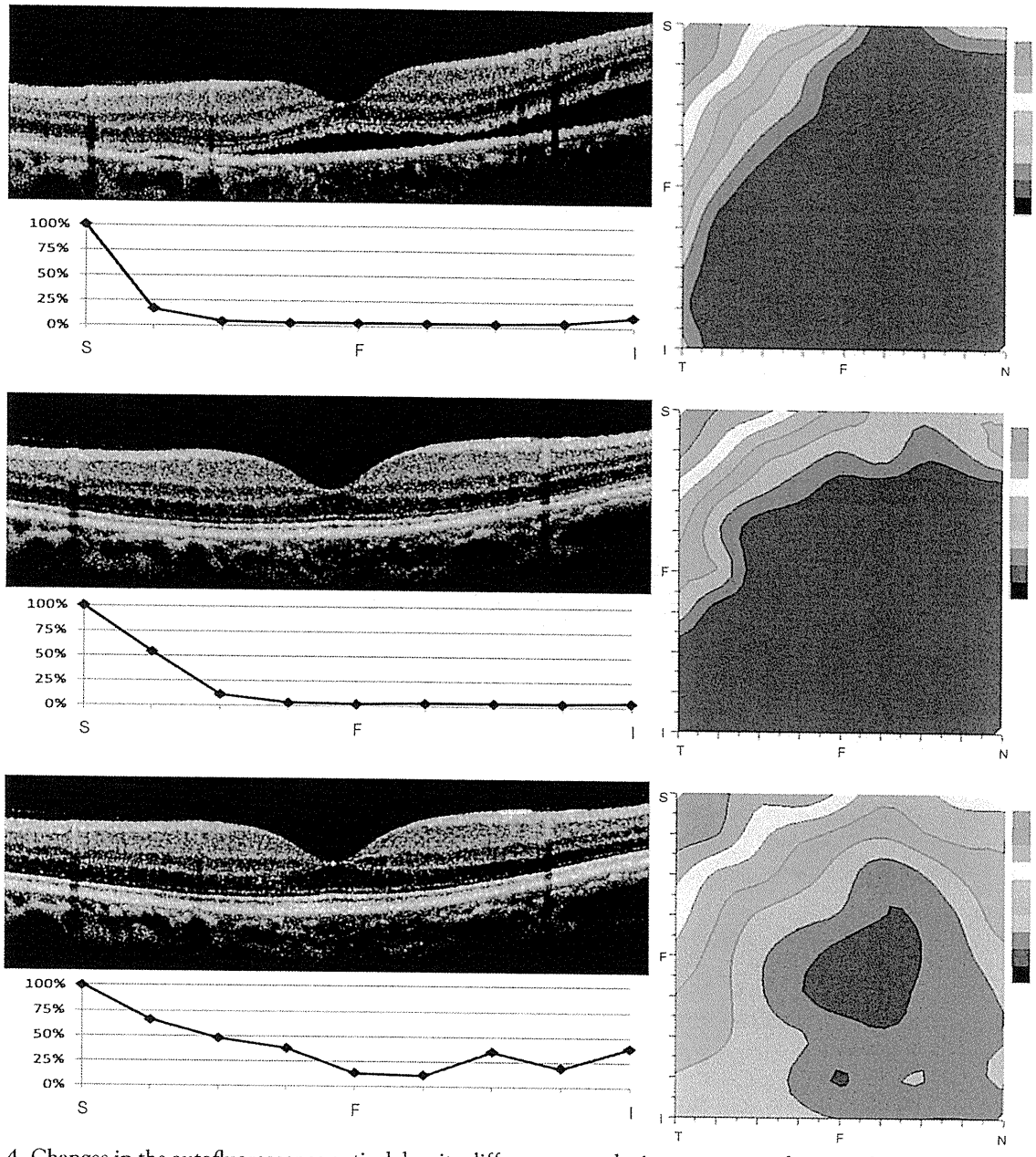

FIGURE 4. Changes in the autofluorescence optical density difference map during acute central serous chorioretinopathy of Patient 1. (Top) Spectral-domain optical coherence tomography (SD-OCT) and autofluorescence densitometry in the acute phase. A vertical SD-OCT scan shows that a serous retinal detachment (SRD) has spread widely within the vascular arcade. Two-dimensional mapping of the autofluorescence optical density difference demonstrates that the concentricity is disrupted. An area of low autofluorescence optical density difference corresponds to the SRD. The % autofluorescence optical density difference graph at the SD-OCT scan line shows that the autofluorescence optical density difference is lower at the SRD than the unaffected area. The abscissa indicates the position: S = superior; F = fovea; I = inferior. (Middle) SD-OCT and autofluorescence densitometry immediately after resolution. The SRD has resolved and the photoreceptor inner and outer segment junction (IS/OS) line disappeared at the affected area on SD-OCT. The concentricity of the autofluorescence optical density difference map did not improve compared to the acute phase. The % autofluorescence optical density difference has not improved at the affected area. (Bottom) Three months after reattachment. The IS/OS line is clearly delineated at the affected area on SD-OCT. The autofluorescence optical density difference map recovers concentricity. The % autofluorescence optical density difference has increased compared with the previous measurement but not to the level of the unaffected area.

intensity inside 9 × 9 grids were measured (Figure 1, Top left). Each grid was 60 × 60 pixels. The autofluorescence optical density difference map showed a normal concentric pattern (Figure 1, Top right). As the wavelength of the excitation light was 488 nm, the map mainly represented the distribution of rhodopsin.[24]

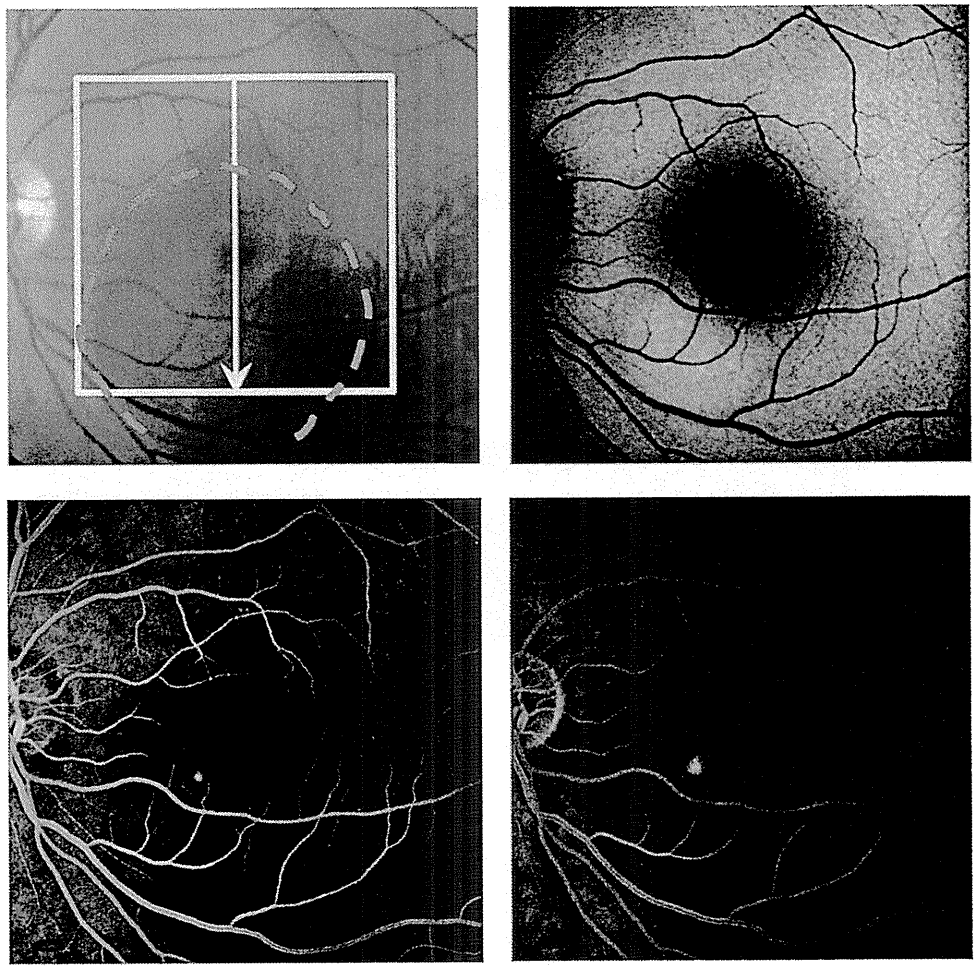

FIGURE 5. Fundus images of the right eye of a 37-year-old man (Patient 4) in the acute phase of central serous chorioretinopathy. (Top left) Fundus photograph. The square indicates the area in which the autofluorescence optical density difference was measured (see Figure 6). The dashed line indicates the serous retinal detachment. The yellow arrow indicates the scanning line of spectral-domain optical coherence tomography (see Figure 6). (Top right) Fundus autofluorescence image. (Bottom) Focal dye leakage is seen in (Bottom left) the early phase and (Bottom right) the late phase of the fluorescein angiograms.

To evaluate the autofluorescence optical density difference at the affected area or to compare SD-OCT findings with autofluorescence optical density difference on the scanned line, we calculated the autofluorescence optical density difference percentage in each grid when the maximum value in the referred area was defined as 100% (% autofluorescence optical density difference). We defined the area in which the % autofluorescence optical density difference was 25% or lower as the low autofluorescence optical density difference area. Figure 1, Bottom shows the % autofluorescence optical density difference along the vertical scan of SD-OCT (Figure 1, Middle) in a representative case.

The photopigments decreased in the detached retina during excitation in acute CSC (Figure 2). Figure 2, Right indicates the time-dependent changes in intensity during light exposure at the corresponding normal area, the SRD, the fovea, and the disc. In the normal area, the retina was bleached and the intensity gradually increased to a plateau. However, the intensity did not increase in the SRD area, indicating a decrease in the photopigments at the detached retina. The intensity remained constant at the fovea and disc.

In the acute phase of eyes with an SRD on SD-OCT, the autofluorescence optical density difference map showed an eccentric pattern in all 16 eyes (Figures 3, 4, 5, and 6). An area of low autofluorescence optical density difference (dense blue) was broader than that in normal eyes, and the area corresponded to the SRD (Figure 4, Top, and Figure 6, Top). An area of high autofluorescence optical density difference (green, yellow, and orange) surrounded the area of low autofluorescence optical density difference. The % autofluorescence optical density difference also showed decrease in intensity corresponding to the area of the SRD on SD-OCT.

Immediately after resolution, the IS/OS was irregular in the area of SRD in 13 eyes and defective in 3 eyes on SD-OCT. In all 16 eyes, the area of low autofluorescence

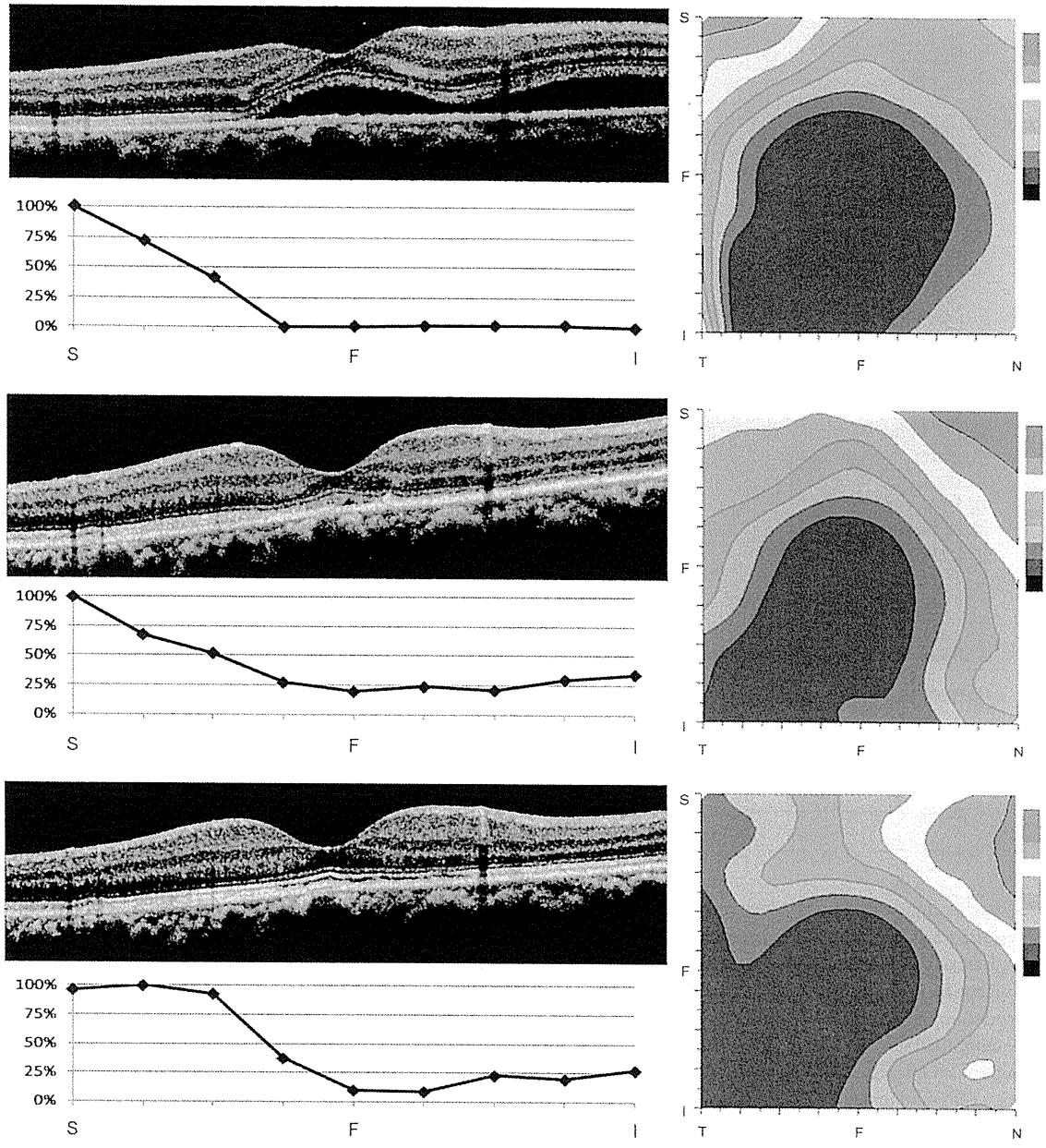

FIGURE 6. Changes in the autofluorescence optical density difference map during acute central serous chorioretinopathy of Patient 4. (Top) Spectral-domain optical coherence tomography (SD-OCT) and autofluorescence densitometry in the acute phase. A vertical SD-OCT scan shows a serous retinal detachment (SRD). Two-dimensional mapping of the autofluorescence optical density difference demonstrates that the concentricity is disrupted. An area of low autofluorescence optical density difference corresponds to the SRD. The % autofluorescence optical density difference graph at the SD-OCT scan line shows that the % autofluorescence optical density difference is lower at the SRD than the unaffected area. The abscissa indicates the position: S = superior; F = fovea; I = inferior. (Middle) SD-OCT and autofluorescence densitometry immediately after reattachment. The SRD has resolved and the photoreceptor inner and outer segment junction (IS/OS) line has disappeared at the affected area on SD-OCT. The autofluorescence optical density difference map has not improved compared to the acute phase. The % autofluorescence optical density difference has not improved at the affected area. (Bottom) Three months after reattachment. The IS/OS line is clearly delineated at the affected area on SD-OCT. The autofluorescence optical density difference mapping has not recovered its concentricity. The % autofluorescence optical density difference has increased compared with the previous measurement but not to the level of the unaffected area.

optical density difference was broader than normal, which was similar to the acute phase (Figure 4, Middle, and Figure 6, Middle). The autofluorescence optical density difference was comparably decreased in eyes with an irregular IS/OS and with a defective IS/OS. The % autofluorescence optical density difference on the same line of the SD-OCT scan also showed the decreased intensity (under 25%) at the reattached retina where the

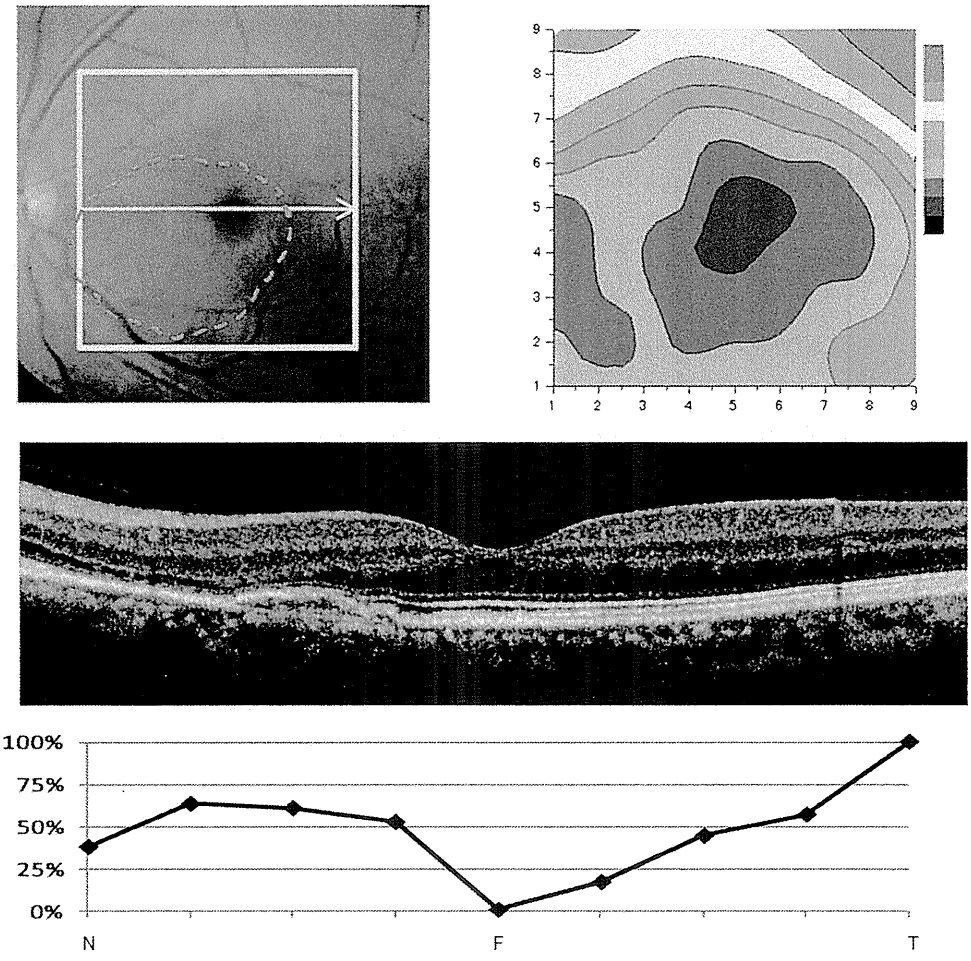

FIGURE 7. Fundus images of the left eye of a 56-year-old man (Patient 5) 3 months after resolution of central serous chorioretinopathy. (Top left) Fundus photograph. The square indicates the area in which the autofluorescence optical density difference was measured. The dashed line indicates the area where serous retinal detachment (SRD) was resolved. The yellow arrow indicates the scanning line of spectral-domain optical coherence tomography (SD-OCT). (Top right) The autofluorescence optical density difference map shows the disruption of concentricity of the photopigment density distribution. An area of low autofluorescence optical density difference corresponds to the affected area. (Middle) The SD-OCT scan shows resolution of serous retinal detachment. The photoreceptor inner and outer segment junction is defected at the reattached area. (Bottom) The % autofluorescence optical density difference graph at the SD-OCT scan line shows that the autofluorescence optical density difference decreased at the affected area. The abscissa indicates the position: N = nasal; F = fovea; T = temporal.

SD-OCT was irregular and the IS/OS was defective immediately after resolution of the SRD.

We performed autofluorescence densitometry and SD-OCT 3 months after resolution in 5 eyes (Patients 1, 2, 3, 4, and 5). Four of the 5 eyes had a clearly delineated IS/OS. One eye had a defective IS/OS (Figure 7). In 2 of the 4 eyes with an IS/OS, the autofluorescence optical density difference map showed improved concentricity and the area of low autofluorescence optical density difference decreased, which indicated recovery of the photopigments (Figure 4, Bottom). The % autofluorescence optical density difference graph showed recovery at the reattached retina. In the other 2 eyes with an IS/OS, the autofluorescence optical density difference map showed eccentricity in the resolved area (Figure 6, Bottom). Although the subretinal fluid resolved and the IS/OS appeared clearly on the SD-OCT images in these 2 eyes, the % autofluorescence optical density difference graph showed lower percentages (under 25%) in the reattached retina compared to the normal area. The autofluorescence optical density difference map and the % autofluorescence optical density difference graph did not show recovery in the 1 eye without an IS/OS (Figure 7).

Figure 8 shows the number of grids of the 81 grids with a low autofluorescence optical density difference in all 16 eyes. There was no significant difference between the acute phase and immediately after resolution in 16 eyes. In the 5 eyes that were reexamined 3 months after resolution, the low autofluorescence optical density difference grids decreased in Cases 1 and 2, and the autofluorescence optical density difference improved in those 2 eyes. The low autofluorescence optical

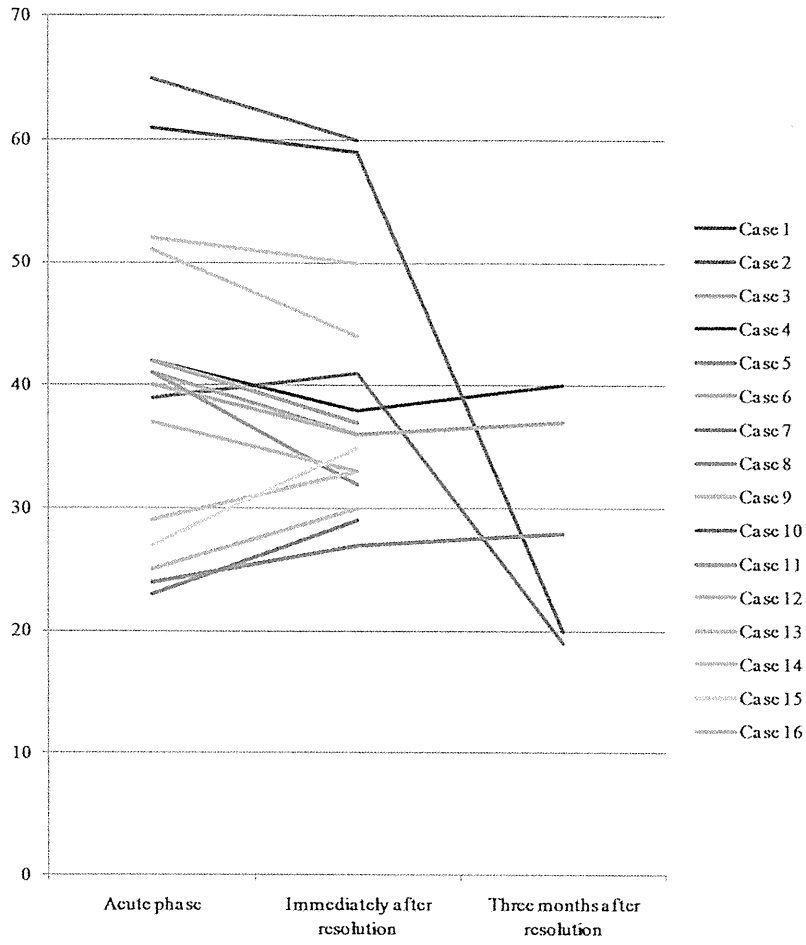

FIGURE 8. The number of grids with low autofluorescence optical density difference of the 81 grids from the 16 cases of central serous chorioretinopathy. The density was measured by autofluorescence densitometry and spectral-domain optical coherence tomography. There is no significant difference between the acute phase and immediately after resolution in all 16 eyes. In the 5 eyes that were reexamined 3 months after resolution, the number of low autofluorescence optical density difference grids has decreased in Cases 1 and 2. The autofluorescence optical density difference has improved in the 2 eyes. The number of low autofluorescence optical density difference grids has not decreased in the other 3 eyes.

density difference grid did not decrease in the other 3 eyes.

The mean best-corrected VA levels in all cases during the acute phase and immediately after resolution were 0.74 and 0.89, respectively. The mean best-corrected VA level was 1.22 in the 5 eyes 3 months after resolution.

DISCUSSION

IN THE CURRENT STUDY, THE PHOTOPIGMENTS WERE EVALuated based on the difference in the distribution of the optical density measured by autofluorescence densitometry in eyes with CSC. The area of the SRD had low autofluorescence optical density difference compared to the unaffected area surrounding the SRD. The area of low autofluorescence optical density difference was almost the same size immediately after resolution of the SRD in all eyes. The autofluorescence optical density difference showed a normal pattern 3 months after resolution of the SRD in 2 eyes. These results suggested that the photopigments decreased in the area of the SRD and did not recover immediately after reattachment.

The VA generally was preserved in CSC despite a retinal detachment. However, many patients with CSC complain of a subjective abnormality in vision such as relative scotoma even after resolution of the SRD. Delayed restoration of the photopigments in CSC has been reported previously.[14,25] Those results were consistent with our observation. However, analysis of the relation of the visual complaint to the morphologic changes was limited before OCT was introduced. Evaluation of the optical density using FAF makes it feasible to analyze the specific distributions of the photopigments and compare them to the SD-OCT findings. SD-OCT has shown various morphologic changes of the outer retina, such as elongation of the outer segments[3] and deposits on the outer retinal surface.[26,27] The results of autofluorescence densitometry suggested a reduction of the photopigments in

TABLE 1. Profiles of Patients With Central Serous Chorioretinopathy

			Acute Phase					Immediately After Resolution				Three Months After Resolution			
Patient No.	Age	Gender	Duration (Months)[a]	Elongation[b]	fODD	BCVA	LP	Time to Resolution (Months)[c]	IS/OS	fODD	BCVA	After Resolution (Months)[d]	IS/OS	fODD	BCVA
1	47	M	2	Yes	↓	1.0	Yes	3	Irregular	No improvement	1.5	3	Clear	Improvement	1.5
2	32	M	2	Yes	↓	0.5	Yes	3	Irregular	No improvement	1.0	3	Clear	Improvement	1.2
3	49	M	4	Yes	↓	1.2	Yes	5	Irregular	No improvement	1.0	3	Clear	No improvement	1.0
4	37	M	2	Yes	↓	0.9	Yes	4	Irregular	No improvement	0.9	3	Clear	No improvement	1.0
5	56	M	7	No	↓	1.2	Yes	10	Defect	No improvement	1.2	3	Defect	No improvement	1.5
6	49	M	1	Yes	↓	1.2	No	6	Irregular	No improvement	1.2	—	—	—	—
7	61	F	1	Yes	↓	0.7	Yes	4	Irregular	No improvement	1.0	—	—	—	—
8	52	F	1	Yes	↓	1.0	No	8	Irregular	No improvement	1.5	—	—	—	—
9	47	M	3	Yes	↓	1.0	Yes	5	Irregular	No improvement	1.5	—	—	—	—
10	43	M	4	Yes	↓	1.0	No	8	Irregular	No improvement	1.5	—	—	—	—
11	63	M	9	Yes	↓	1.2	Yes	13	Irregular	No improvement	1.2	—	—	—	—
12	48	M	31	Yes	↓	0.9	Yes	32	Irregular	No improvement	1.0	—	—	—	—
13	56	M	61	No	↓	0.4	Yes	64	Defect	No improvement	0.5	—	—	—	—
14	59	M	46	No	↓	0.3	Yes	54	Defect	No improvement	0.2	—	—	—	—
15	31	M	4	No	↓	0.3	No	6	Irregular	No improvement	0.4	—	—	—	—
16	71	M	49	No	↓	0.4	Yes	50	Irregular	No improvement	0.6	—	—	—	—
Mean	50.1		14.2			0.74		17.2			0.89				1.22
SD	11.0		20.3					20.6							

↓ = decreased; BCVA = best-corrected visual acuity; F = female; fODD = autofluorescence optical density difference; IS/OS = photoreceptor inner and outer segment junction; LP = laser photocoagulation; M = male; SD = standard deviation.

[a]Duration of symptom from onset.

[b]Elongation of photoreceptor outer segment.

[c]Duration from onset to confirmation of resolution.

[d]Period from resolulition to examination.

the area of the SRD, even though the photoreceptors elongated in the outer retina (Figure 4). The density of the photopigments may decrease in the elongated outer segments. Reduction of the retinal derivatives and related protein as a result of dilution has been presumed to occur in the subretinal space in eyes with CSC.[14,25] The photoreceptor cells produce the outer segments that contain very few photopigments in the retina of retinoid-deprived rats.[28] Engbretson and Witkovsky[29] reported that the rod outer segments grow normally in severely vitamin A–deficient Xenopus tadpoles. Previous reports and the results of the current study indicate that the photoreceptor cells may continue to produce outer segments that contain few photopigments in eyes with an SRD.

After retinal reattachment, the IS/OS lines on the OCT images were irregular in most eyes with CSC (Table), which suggested 2 possibilities. One is the actual loss of the outer segments, and another is decreased signal intensity attributable to misalignment or disorientation of the outer segments. The Stiles-Crawford effect should be considered in retinal densitometry.[16] However, as orientation of the photoreceptors had little effect on optical density changes measured by FAF,[30] autofluorescence densitometry could measure the density of the photopigments despite the fact that the outer segment was not aligned. Therefore, the former possibility is likely. Namely, the disappearance of the IS/OS immediately after resolution in CSC suggests that the outer segments may be phagocytized or absorbed after reattachment, which is consistent with the finding of shortened outer segments after retinal reattachment in experimental retinal detachments.[31] However, the mechanism of the disappearance of the outer segments is unknown. The renewal rate of the rod outer segments in rat eyes decreased after retinal reattachment because of photoreceptor dysfunction,[32] which causes shortening of the outer segment if the shedding of the discs occurs at a normal rate. Impairment of the photoreceptor cells after resolution of SRD in CSC has been proved electrophysiologically.[11,15] The function of the photoreceptor cells may be involved in the disappearance of the outer segments.

Long-standing macular dysfunction has been reported in recent clinical or electrophysiologic studies.[8,10,12,33] Delayed restoration of the photopigments may contribute to macular dysfunction because vitamin A deprivation impairs retinal sensitivity.[34,35] However, the relationship between the density of the photopigments and retinal sensitivity is not seen clearly in eyes with CSC. Further studies are needed to understand this. Photoreceptor apoptosis should be considered to investigate visual function in CSC, since apoptosis has been reported in experimental retinal detachment and human retinal detachment within a few days.[31,36,37]

Eyes with an irregular IS/OS immediately after resolution of a SRD had fewer photopigments corresponding to the area of the irregular IS/OS on the autofluorescence optical density difference map. Two of the 5 eyes that recovered a clearly delineated IS/OS had a normal autofluorescence optical density difference distribution 3 months after resolution of the SRD. The findings of the IS/OS on OCT images corresponded to the status of the photopigments measured by autofluorescence densitometry. However, the autofluorescence optical density difference and the % autofluorescence optical density difference did not improve in 2 eyes with a clearly delineated IS/OS 3 months after resolution of the SRD (Figure 6), suggesting that a well-delineated IS/OS line indicates photopigment formation but does not assure a normal concentration of photopigments in the outer segments. This result may reflect relative scotoma after resolution of SRD. Since the outer segment discs were synthesized in vitamin A–deprived animals,[28,38] few photopigments containing outer segments may be produced in human eyes. Since a reduction of the photopigments in eyes without pathologic changes in aged individuals has been reported,[39,40] photopigments may decrease in aged persons with normal IS/OS findings. Further studies are needed.

The current study had several weaknesses, including a small number of cases and short follow-up time. It is difficult to evaluate the absolute value of the density of the photopigments, because HRA2 does not have apparatus to determine the laser intensity to expose photopigments and the rate of attenuation of autofluorescence from the fundus. As a result, the autofluorescence optical density difference could not be compared directly among the cases. Since the autofluorescence densitometry in our technique primarily measures the rod photopigments, the data are unsuitable for assessing the photopigments at the fovea. With regard to the light absorbance characteristics, autofluorescence optical density difference may be affected by macular pigments and cone photopigments. Because of absorption by the macular pigment, the AF signal is low at the fovea. Therefore no differences of AF intensity can be observed between bleached and unbleached state. We could observe the decline of photopigments and related functional impairment in the area of SRD except for the fovea. Although most subjective vision complaints are about central vision, abnormalities of parafoveal and perifoveal function, which can be detected by our technique, also affect subjective symptoms. These problems may be overcome by using a longer light source for the measurements. On the other hand, recent research reported that quantitative measurement of FAF can be performed with HRA2 modified by insertion of a fluorescence reference chip (Duncker T, et al. IOVS 2010;51:ARVO E-Abstract 262). Quantitative measurement of photopigment might be achieved using this method in combination with autofluorescence densitometry.

In conclusion, we observed reduction and recovery of photopigments in CSC under different conditions. We think that autofluorescence densitometry can evaluate retinal function based on the changes in the photopigments in CSC figures 3 and 5.

THE AUTHORS INDICATE NO FINANCIAL SUPPORT OR NO FINANCIAL CONFLICT OF INTEREST. INVOLVED IN DESIGN AND conduct of study (A.O., T.I., T.S.); collection (A.O., I.M., Y.S.), management, analysis, and interpretation of data (A.O., T.I., T.S., I.M.); and preparation and review (A.O., T.I.) and approval of the manuscript (A.O., T.I., T.S., I.M., Y.S.). This study followed the tenets of the Declaration of Helsinki. The institutional review board at Fukushima Medical University School of Medicine approved: 1) observation using OCT and autofluorescence densitometry for eyes with macular and retinal disorder; 2) the observational study for CSC and its similar disorders at the treatment and follow-up; and 3) the prospective comparative analysis performed in this study.

REFERENCES

1. Maruko I, Iida T, Sekiryu T, Saito M. Morphologic changes in the outer layer of the detached retina in rhegmatogenous retinal detachment and central serous chorioretinopathy. Am J Ophthalmol 2009;147(3):489–494 e1.
2. Piccolino FC, de la Longrais RR, Ravera G, et al. The foveal photoreceptor layer and visual acuity loss in central serous chorioretinopathy. Am J Ophthalmol 2005;139(1):87–99.
3. Matsumoto H, Kishi S, Otani T, Sato T. Elongation of photoreceptor outer segment in central serous chorioretinopathy. Am J Ophthalmol 2008;145(1):162–168.
4. Ojima Y, Hangai M, Sasahara M, et al. Three-dimensional imaging of the foveal photoreceptor layer in central serous chorioretinopathy using high-speed optical coherence tomography. Ophthalmology 2007;114(12):2197–2207.
5. Iida T, Hagimura N, Sato T, Kishi S. Evaluation of central serous chorioretinopathy with optical coherence tomography. Am J Ophthalmol 2000;129(1):16–20.
6. Furuta M, Iida T, Kishi S. Foveal thickness can predict visual outcome in patients with persistent central serous chorioretinopathy. Ophthalmologica 2009;223(1):28–31.
7. Iida T, Yannuzzi LA, Spaide RF, Borodoker N, Carvalho CA, Negrao S. Cystoid macular degeneration in chronic central serous chorioretinopathy. Retina 2003;23(1):1–7; quiz 137–138.
8. Matsumoto H, Sato T, Kishi S. Outer nuclear layer thickness at the fovea determines visual outcomes in resolved central serous chorioretinopathy. Am J Ophthalmol 2009;148(1):105–110 e1.
9. Ozdemir H, Karacorlu SA, Senturk F, Karacorlu M, Uysal O. Assessment of macular function by microperimetry in unilateral resolved central serous chorioretinopathy. Eye (Lond) 2008;22(2):204–208.
10. Ojima Y, Tsujikawa A, Hangai M, et al. Retinal sensitivity measured with the micro perimeter 1 after resolution of central serous chorioretinopathy. Am J Ophthalmol 2008;146(1):77–84.
11. Vajaranant TS, Szlyk JP, Fishman GA, Gieser JP, Seiple W. Localized retinal dysfunction in central serous chorioretinopathy as measured using the multifocal electroretinogram. Ophthalmology 2002;109(7):1243–1250.
12. Suzuki K, Hasegawa S, Usui T, et al. Multifocal electroretinogram in central serous chorioretinopathy. Jpn J Ophthalmol 2000;44(5):571.
13. Theelen T, Berendschot TT, Boon CJ, Hoyng CB, Klevering BJ. Analysis of visual pigment by fundus autofluorescence. Exp Eye Res 2008;86(2):296–304.
14. van Meel GJ, Smith VC, Pokorny J, van Norren D. Foveal densitometry in central serous choroidopathy. Am J Ophthalmol 1984;98(3):359–368.
15. Miyake Y, Shiroyama N, Ota I, Horiguchi M. Local macular electroretinographic responses in idiopathic central serous chorioretinopathy. Am J Ophthalmol 1988;106(5):546–550.
16. DeLint PJ, Berendschot TT, van Norren D. A comparison of the optical Stiles-Crawford effect and retinal densitometry in a clinical setting. Invest Ophthalmol Vis Sci 1998;39(8):1519–1523.
17. Alpern M, Pugh EN Jr. The density and photosensitivity of human rhodopsin in the living retina. J Physiol 1974;237(2):341–370.
18. Rushton WA, Campbell FW. Measurement of rhodopsin in the living human eye. Nature 1954;174(4441):1096–1097.
19. van Norren D, van der Kraats J. A continuously recording retinal densitometer. Vision Res 1981;21(6):897–905.
20. Liem AT, Keunen JE, van Norren D, van de Kraats J. Rod densitometry in the aging human eye. Invest Ophthalmol Vis Sci 1991;32(10):2676–2682.
21. Tornow RP, Stilling R, Zrenner E. Scanning laser densitometry and color perimetry demonstrate reduced photopigment density and sensitivity in two patients with retinal degeneration. Vision Res 1999;39(21):3630–3641.
22. Burns SA, Eisner AE, Lobes LA Jr. Foveal cone photopigment bleaching in central serous retinopathy. Appl Opt 1988;27(6):1045–1049.
23. Liem AT, Keunen JE, Van Norren D. Clinical applications of fundus reflection densitometry. Surv Ophthalmol 1996;41(1):37–50.
24. Sekiryu T, Iida T, Maruko I, Horiguchi M. Clinical application of autofluorescence densitometry using a scanning laser ophthalmoscope. Invest Ophthalmol Vis Sci 2009;50(6):2994–3002.
25. Chuang EL, Sharp DM, Fitzke FW, Kemp CM, Holden AL, Bird AC. Retinal dysfunction in central serous retinopathy. Eye 1987;1(Pt 1):120–125.
26. Spaide RF, Klancnik JM Jr. Fundus autofluorescence and central serous chorioretinopathy. Ophthalmology 2005;112(5):825–833.
27. Kon Y, Iida T, Maruko I, Saito M. The optical coherence tomography-ophthalmoscope for examination of central serous chorioretinopathy with precipitates. Retina 2008;28(6):864–869.
28. Katz ML, Kutryb MJ, Norberg M, Gao CL, White RH, Stark WS. Maintenance of opsin density in photoreceptor outer segments of retinoid-deprived rats. Invest Ophthalmol Vis Sci 1991;32(7):1968–1980.
29. Engbretson GA, Witkovsky P. Rod sensitivity and visual pigment concentration in Xenopus. J Gen Physiol 1978;72(6):801–819.
30. Prieto PM, McLellan JS, Burns SA. Investigating the light absorption in a single pass through the photoreceptor layer by means of the lipofuscin fluorescence. Vision Res 2005;45(15):1957–1965.

31. Lewis GP, Charteris DG, Sethi CS, Leitner WP, Linberg KA, Fisher SK. The ability of rapid retinal reattachment to stop or reverse the cellular and molecular events initiated by detachment. Invest Ophthalmol Vis Sci 2002;43(7):2412–2420.
32. Guerin CJ, Lewis GP, Fisher SK, Anderson DH. Recovery of photoreceptor outer segment length and analysis of membrane assembly rates in regenerating primate photoreceptor outer segments. Invest Ophthalmol Vis Sci 1993;34(1):175–183.
33. Baran NV, Gurlu VP, Esgin H. Long-term macular function in eyes with central serous chorioretinopathy. Clin Experiment Ophthalmol 2005;33(4):369–372.
34. Kemp CM, Jacobson SG, Borruat FX, Chaitin MH. Rhodopsin levels and retinal function in cats during recovery from vitamin A deficiency. Exp Eye Res 1989;49(1):49–65.
35. Kemp CM, Jacobson SG, Faulkner DJ, Walt RW. Visual function and rhodopsin levels in humans with vitamin A deficiency. Exp Eye Res 1988;46(2):185–197.
36. Cook B, Lewis GP, Fisher SK, Adler R. Apoptotic photoreceptor degeneration in experimental retinal detachment. Invest Ophthalmol Vis Sci 1995;36(6):990–996.
37. Arroyo JG, Yang L, Bula D, Chen DF. Photoreceptor apoptosis in human retinal detachment. Am J Ophthalmol 2005;139(4):605–610.
38. Herron WL Jr, Riegel BW. Production rate and removal of rod outer segment material in vitamin A deficiency. Invest Ophthalmol 1974;13(1):46–53.
39. Curcio CA, Millican CL, Allen KA, Kalina RE. Aging of the human photoreceptor mosaic: evidence for selective vulnerability of rods in central retina. Invest Ophthalmol Vis Sci 1993;34(12):3278–3296.
40. Elsner AE, Burns SA, Beausencourt E, Weiter JJ. Foveal cone photopigment distribution: small alterations associated with macular pigment distribution. Invest Ophthalmol Vis Sci 1998;39(12):2394–2404.

SUBFOVEAL CHOROIDAL THICKNESS AFTER TREATMENT OF VOGT–KOYANAGI–HARADA DISEASE

ICHIRO MARUKO, MD,* TOMOHIRO IIDA, MD,* YUKINORI SUGANO, MD,* HIROSHI OYAMADA, MD,* TETSUJU SEKIRYU, MD,* TAKAMITSU FUJIWARA, MD,† RICHARD F. SPAIDE, MD‡

Purpose: To evaluate the subfoveal choroidal thickness in Vogt–Koyanagi–Harada (VKH) disease using enhanced depth imaging optical coherence tomography.

Methods: Retrospective observational study. Subfoveal choroidal thickness was measured using enhanced depth imaging optical coherence tomography, in which the optical coherence tomography instrument was placed close enough to the eye to obtain an inverted image, which was averaged for 100 scans. All patients were diagnosed as having the ocular findings of VKH disease with or without extraocular disorders. The patients were followed during their initial treatment with corticosteroids.

Results: All 8 patients (16 eyes) with acute phase VKH disease presented with thickening of the choroid. The serous retinal detachment disappeared in 1 month after corticosteroid treatment. The mean choroidal thickness in 16 eyes decreased from 805 ± 173 μm at the first visit to 524 ± 151 μm at 3 days ($P < 0.001$) and 341 ± 70 μm by 2 weeks ($P < 0.001$).

Conclusion: Patients with active VKH disease have markedly thickened choroids, possibly related not only to inflammatory infiltration but also to increased exudation. Both the choroidal thickness and the exudative retinal detachment decreased quickly with corticosteroid treatment. Enhanced depth imaging optical coherence tomography can be used to evaluate the choroidal involvement in VKH disease in the acute stages and may prove useful in the diagnosis and management of this disease noninvasively.

RETINA 31:510–517, 2011

Vogt–Koyanagi–Harada (VKH) disease is a bilateral granulomatous uveitis characterized by the iridocyclitis and exudative retinal detachment in the acute stage. Although the extraocular manifestations in VKH disease are also reported such as meningismus, tinnitus, perception deafness, cerebrospinal fluid pleocytosis, alopecia, poliosis of the eyebrow, eyelashes and scalp hair, and depigmentation of skin,[1,2] some patients with only ocular findings are diagnosed as probable or incomplete VKH disease according to its criteria.

Ocular findings of VKH disease, including probable and incomplete cases,[2] show the following characteristics independent of any extraocular disorders: in the acute stage, fluorescein angiography shows multifocal leaks from the level of retinal pigment epithelium (RPE) with later multilobular pooling of dye within multiple serous retinal detachments. Indocyanine green angiography shows patchy filling delays and blockage by subretinal fluid with hypofluorescent spots with interspersed areas of increased fluorescence and indistinct visualization of choroidal vessels, which are often seen throughout all phases, and there can be late segmental staining of choroidal vessels.[3–7] Optical coherencetomography (OCT) shows partitioned subretinal fluid with associated intraretinal edema.[8–11] In the chronic

From the *Department of Ophthalmology, School of Medicine, Fukùshima Medical University, Fukushima, Japan; †Department of Ophthalmology, School of Medicine, Iwate Medical University, Morioka, Japan; and ‡Vitreous Retina Macula Consultants of New York, New York, New York.

The authors have no proprietary or commercial interest in any materials discussed in this article.

Reprint requests: Ichiro Maruko, MD, Department of Ophthalmology, School of Medicine, Fukushima Medical University, 1 Hikarigaoka, Fukushima, 960-1295, Japan; e-mail: imaruko@fmu.ac.jp

and remission stage, a sunset glow fundus, peripheral atrophy, and scarring of the RPE are observed.

Vogt–Koyanagi–Harada disease is a common form of uveitis in Asia, especially in Japan.[1,2,12,13] Vogt–Koyanagi–Harada disease appears to originate from the choroid. Evaluating the choroidal involvement has potential importance for assessing treatment efficacy and recurrence in VKH disease. Indocyanine green angiography enables visualization of the choroidal vessels; however, it limited the utility for VKH disease because diagnostic characteristics include the blurred visualization of choroid. Also, indocyanine green angiography is invasive and inconvenient to perform repeatedly during the course of a patient's follow-up. B-mode ultrasonographic imaging is capable of demonstrating more marked amounts of choroidal thickening[14,15]; however, the resolution of conventional ultrasonography is orders of magnitude less than that of OCT. Recently, a new method for the evaluation of the choroid was developed and called enhanced depth imaging OCT (EDI-OCT).[16] In the current study, we observed the morphologic choroidal change during the treatment in the acute stage of ocular finding of VKH disease using EDI-OCT.

Methods

This retrospective study followed the tenets of the Declaration of Helsinki. The Institutional Review Board at the Fukushima Medical University School of Medicine and the Iwate Medical University approved the observation and the retrospective comparative analysis using OCT for eyes with macular and retinal disorders.

Each patient had a complete ophthalmic examination to include indirect ophthalmoscopy, slit-lamp biomicroscopy with a contact lens, and digital fluorescein and indocyanine green angiography (TRC-50IX/IMAGEnet H1024 system; Topcon, Tokyo, Japan). The patients had best-corrected visual acuity measurements that were obtained with a Japanese standard decimal visual chart and calculated by logarithm of the minimum angle of resolution scale for comparing the mean best-corrected visual acuity. All eyes were examined by the Heidelberg Spectralis OCT (Heidelberg Engineering, Heidelberg, Germany) with eye tracking and image averaging systems. The vertical and horizontal scans were obtained at each measurement to evaluate the center of fovea precisely. Follow-up function with Spectralis OCT software was used to avoid measuring the different position with first examination.

Table 1. The Clinical Changes of Choroidal Thickness and Height of Serous Retinal Detachment During the Follow-up Periods in VKH Disease

Patient	Age	Gender*	Diagnosis	Meningismus	Auditory Findings	Integumentary	Eye	Type	Choroidal Thickness (μm)					Height of SRD (μm)				
									Baseline	Day 1	Day 3	Day 7	Day 14	Baseline	Day 1	Day 3	Day 7	Day 14
1	30	M	Incomplete	Yes	Deafness	None	OD	SRD	1,000†	721	695	499	341	647	209	194	143	0
							OS	SRD	1,000†	1,000†	690	543	355	1,234	146	186	119	0
2	54	M	Incomplete	Yes	Deafness	None	OD	SRD	872	782	639	452	318	115	184	173	194	86
							OS	SRD	843	720	626	428	325	165	177	81	104	57
3	41	F	Incomplete	Yes	Deafness	None	OD	SRD	612	568	—	415	413	786	616	—	102	24
							OS	SRD	576	555	—	484	392	522	247	—	57	0
4	17	F	Incomplete	Yes	Tinnitus	None	OD	SRD	656	577	412	319	266	345	150	131	126	0
							OS	Papillitis	570	440	308	259	233	0	0	0	0	0
5	51	F	Incomplete	Yes	Tinnitus	None	OD	SRD	955	805	509	421	396	208	188	186	87	0
							OS	SRD	963	774	451	404	371	263	210	163	112	0
6	22	F	Incomplete	Yes	None	None	OD	SRD	1,000†	975	762	569	465	847	825	529	213	0
							OS	SRD	1,000†	930	627	531	443	776	689	324	101	0
7	41	M	Incomplete	NA	Tinnitus	None	OD	SRD	681	571	445	335	306	72	74	59	30	0
							OS	SRD	876	688	523	405	328	163	187	133	72	0
8	35	F	Probable	NA	None	None	OD	SRD	649	550	339	278	261	189	134	72	44	0
							OS	SRD	634	461	311	250	245	200	172	50	0	0
Mean ± SD	36.4	—	—	—	—	—	—	—	805 ± 173	695 ± 175	524 ± 151	412 ± 101	341 ± 70	408 ± 352	263 ± 232	163 ± 133	94 ± 60	10
																		25

Choroidal thickness measured using the spectral-domain EDI-OCT technique.
*Male to female ratio was 3:5.
†These are defined as a 1,000 μm because the inner scleral border cannot be visualized when choroidal thickness values become more than 1,000 μm.
NA, not available; Deafness, perceptive deafness; SRD, serous retinal detachment type of VKH disease; Papillitis, papillitis type of VKH disease.